Available online at www.sciencedirect.com
SCIENCE DIRECT®
Journal of Electron Spectroscopy and Related Phenomena 150 (2006) 220–227
JOURNAL OF ELECTRON SPECTROSCOPY and Related Phenomena
www.elsevier.com/locate/elspec

Cytochrome *c* interaction with hematite (α-Fe_2O_3) surfaces

Carrick M. Eggleston *, Nidhi Khare, David M. Lovelace

Department of Geology and Geophysics, University of Wyoming, Laramie, WY 82071, USA

Available online 16 September 2005

Abstract

The interaction of metalloproteins such as cytochromes with oxides is of interest for a number of reasons, including molecular catalysis of environmentally important mineral-solution electron transfer reactions (e.g., dehalogenations) and photovoltaic applications. Iron reduction by bacteria, thought to be cytochrome mediated, is of interest for geochemical and environmental remediation reasons. As a baseline for understanding cytochrome interaction with ferric oxide surfaces, we report on the interaction of mitochondrial cytochrome *c* (Mcc), a well-studied protein, with hematite (α-Fe_2O_3) surfaces. Mcc sorbs strongly to hematite from aqueous solution in a narrow pH range corresponding to opposite charge on Mcc and hematite (between pH 8.5 and 10, Mcc is positively charged and hematite surfaces are negatively charged). Cyclic voltammetry of Mcc using hematite electrodes gives redox potentials characteristic of Mcc in a native conformational state, with no evidence for unfolding on the hematite surface. Atomic force microscopy imaging is consistent with a loosely attached adsorbate that is easily deformed by the AFM tip. In phosphate-containing solution, Mcc adhers to the surface more strongly. These results establish hematite as a viable material for electrochemical and spectroscopic characterization of cytochrome–mineral interaction.

Keywords: Hematite; Iron oxide; Cytochrome; Adsorption; Voltammetry; AFM

1. Introduction

The interaction of proteins with minerals is relevant to a variety of emerging fields. The biochemical pathways that lead to synthesis of heme proteins evolved very early in the history of life, and must have involved a system for iron acquisition and incorporation [1,2]. There is growing interest in the use of redox metalloproteins, separately from living systems, as redox catalysts or mediators. Cytochromes and other molecules are under study as catalysts for reductive dehalogenation reactions in environmental applications [3]; as part of understanding how such a process might work, researchers have tested ideas about how physiological redox partners (e.g., cytochrome oxidases and reductases) might be replaced with inorganic substances such as oxide electrodes [4]. Redox metalloproteins such as cytochromes have been applied, in conjunction with iron oxide and other electrodes, as biosensors [5–7]. The cytochrome *c* used in the present study, as well as derivatives, have been used as adsorbed sensitizers on nanocrystalline TiO_2 films for photovoltaic applications [8–10].

There is also interest in the use of metal-reducing bacteria to reductively immobilize metal and radionuclide contaminants [11–13], and there remains the possibility that redox catalyst proteins, separate from whole organisms, could be of utility in such applications. In this context, the interaction of a relatively inexpensive and well-studied cytochrome with mineral surfaces is of interest because (a) it provides a useful comparative baseline for understanding other cytochromes' interactions with these surfaces and (b) because it may itself be of direct use in mineral-solution interfacial redox catalysis.

Beyond these specific applications, interactions between microorganisms and minerals are fundamental to the operation of the natural world. Plants grow in soils that constitute physically, chemically, and biologically complex bioreactors involving inorganic mineral substrates, microorganisms, and higher plants and animals. There is a growing understanding of the geochemical roles played by early microorganisms and later by photosynthetic organisms in creating the environment on earth that we, and other multicellular forms of life, enjoy (and must increasingly protect) [14–17]. There are minerals (e.g., pyrite, magnetite, biotite, others) that serve as oxidizable energy sources for organisms, and other minerals (e.g., ferric and manganese oxides and hydroxides) that can be used as respiratory electron acceptors in environments deprived of oxygen [16].

* Corresponding author. Tel.: +1 307 766 6769; fax: +1 307 766 6769.
E-mail address: carrick@uwyo.edu (C.M. Eggleston).

0368-2048/$ – see front matter © 2005 Elsevier B.V. All rights reserved.
doi:10.1016/j.elspec.2005.06.006

Cytochromes have been implicated in microbe-mineral electron transfer [18–22].

This paper presents results for the interaction of mitochondrial cytochrome *c* (Mcc) with iron oxide surfaces and compares them to previous results for interaction of this and other cytochromes with oxides. Although previous research has dealt with tin and indium oxide electrodes [23,24], TiO_2 nanoparticle films [7–10], and clay-modified graphite electrodes [25], this is the first report to our knowledge of the direct electrochemistry of Mcc on an iron oxide electrode as well as the first AFM-imaging and study of pH-dependent adsorption on iron oxide.

2. Mcc background

We used horse heart cytochrome *c* (PDB ID: 1HRC) from Sigma, a mitochondrial cytochrome *c*. Mcc was among the first redox proteins to be purified and studied [26]; its amino acid composition, basic conformational states, redox potentials, and isoelectric point were known by 1941 [27]. Mcc is a globular protein (12.4 kDa, 3.4 nm diameter) consisting of 104 amino acid residues in a single polypeptide chain and a covalently attached heme group. It contains 19 lysine residues, of which Lys 13, 27, 72 and 79 are grouped around the heme edge of the molecule (Fig. 1A). The high lysine content gives Mcc an isoelectric point (IEP) of about pH 10 [28]. The charge distribution is inhomogenous (Fig. 1B), imparting a dipole moment of 308 and 325 D for the reduced and oxidized forms, respectively, at neutral pH [29]. The dipole moment is a key factor in the orientation and docking of Mcc with its oxidase and reductase [30]. The heme Fe is axially coordinated by histidine 18 and methionine 80, and is maintained in the low-spin state in the native conformation. The most easily broken axial bond (to the S in methionine 80) is disrupted at extreme pH or elevated temperature, and can be replaced by ligands such as CN^-, N_3^-, or imidazole. The breaking of the Fe–S bond results in switching to the high spin state, and allows a portion of the polypeptide chain (from residue 78 to residue 90) to move away from the heme and expose the heme to a more aqueous environment that is thought to promote electron transfer from the reduced heme to electron acceptors [28].

Using redox mediators, the native redox potential of Mcc has been measured at +0.04 to +0.07 V versus Ag/AgCl [31,32]. In 1977, two groups performed direct electrochemistry with Mcc using solid electrodes. Reversible redox peaks at near-native potentials were obtained if the Mcc was stabilized with a co-adsorbed layer of 4,4′-bipyridine [33], and Yeh and Kuwana [23] obtained reversible redox waves using an indium-doped tin oxide electrode. Later it was shown that a number of other co-adsorbed molecules would also stabilize Mcc, including a layer of adsorbed phosphate [34].

Bowden et al. [24] showed that reversible or irreversible behavior could be produced depending on the surface treatment of the oxide electrode and on pH. They found a slight (15 mV) negative shift of the Mcc redox potential on indium oxide electrodes as compared to tin oxide electrodes, and pointed out that this shift is comparable to those measured when the molecule interacts with phospholipids, mitochondria, and other isolated enzymes. Mcc interaction with hematite electrodes, then, might show a similarly small shift (compared to tin oxide) and still be considered “native”. Chen et al. [32] showed, using functionalized alkanethiol self-assembled monolayers (SAMs) on gold electrodes, that SAMs terminated with hydrophilic terminal groups (e.g., carboxyls), or even methyl groups attached to N^+ centers, near-native redox potentials were observed. SAMs with methyl-terminated alkanes, however, gave a redox potential of −320 mV versus Ag/AgCl. This potential is close to that of “bare” heme, with no protein wrapping, on similarly functionalized electrodes [35] and has been interpreted as an indication that the Mcc has unfolded to expose the heme. We would expect that, if Mcc unfolds on hematite electrodes, that we would observe a similarly large shift in redox potential.

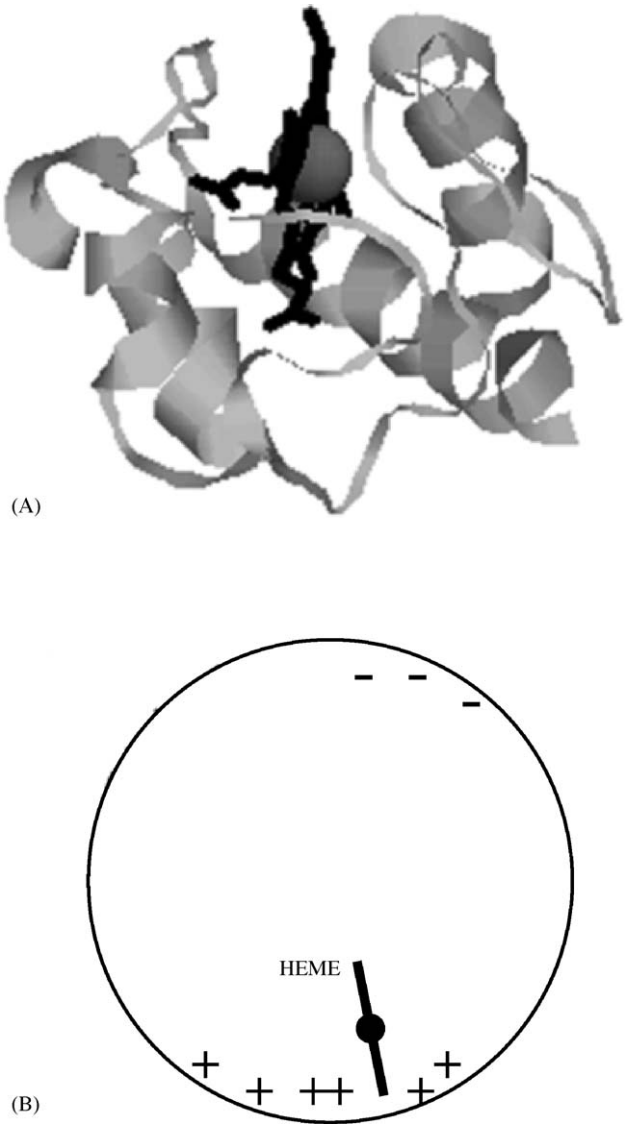

Fig. 1. (A) RASMOL rendering of Mcc (PDB ID: 1HRC) with the protein in gray, the heme in black, and the Fe of the heme a dark gray sphere. The heme occupies a “groove” that can open to solvent if axial bonding to Fe is severed. (B) Cartoon of Mcc showing positive charge associated with the heme groove and an electric dipole.

Another factor in controlling the electrochemical behavior of Mcc is its orientation. Fig. 1 shows that the electroactive Fe in the heme is close to the positively charged edge of the Mcc molecule; in the absence of wholesale unfolding, the heme would be expected to achieve best electronic overlap with electrode states when the electrode surface is negatively charged, orienting the positively charged lysine-rich heme groove toward the surface. It has been noted that, for Mcc separated from a gold electrode by varying chain lengths of carboxy-terminated alkane thiols, chain lengths of 8 or less result in distance-independent electron transfer rates [36]. This result is contrary to tunneling theory, and indicates that another process is rate limiting at low separations. The rate-limiting factor is thought to be conformational change in the protein that promotes (or allows) electron transfer [36].

There have been a few studies of polyheme bacterial membrane cytochrome interaction with aqueous Fe(III) complexes and mineral-modified electrodes. Lojou et al. [37] studied the catalytic reduction of aqueous Fe(III) citrate by various mono- and polyheme cytochromes reduced at poly-L-lysine-modified graphite electrodes. Mcc, with the most positive reduction potential of the cytochromes studied, did not catalyze Fe(III) citrate reduction, whereas polyheme cytochromes obtained form sulfur and sulfate reducing bacteria were effective. Although these cytochromes had widely differing isoelectric points (10.2–4.8), they were comparably effective in Fe(III) citrate reduction. A shared characteristic in the tested cytochrome was bihistidine axial Fe coordination of heme Fe, as opposed to histidine–methionine axial Fe coordination in Mcc. Such cytochromes have a more negative reduction potential. Lojou et al. [38] extended previous work by showing that outer membrane bacterial cytochromes could catalyze electron transfer to Fe(III) oxyhydroxides. Magnuson et al. [39] showed the same to be true of OmcC, an outer membrane cytochrome from *Geobacter sulfurreducens*. However, neither of these studies report direct electrochemistry of bacterial cytochromes using iron oxide electrodes.

Sallez et al. [25] studied the interaction between Mcc and polyheme cytochromes from sulfate reducing bacteria using pyrolytic graphite (PG) electrodes modified with clay coatings, including electroinactive minerals such as kaolinite and montmorillonite as well as electroactive goethite (α-FeOOH). The electroinactive clays tended simply to screen the PG electrode from the cytochromes, but CV currents were greater on goethite-modified electrodes than on bare PG electrodes. CV of Mcc on goethite-coated PG electrodes suggested that Mcc retains near-native conformation in the presence of goethite, and that the goethite helps attract cytchrome to the electrode, but the electrochemical response does not reflect direct electrochemistry (electron transfer) between goethite and cytochrome. Some polyheme cytochromes exhibited large cathodic peaks but small or absent anodic peaks, suggesting that these cytochromes catalyzed goethite reduction. The present study is the first, to our knowledge, of direct electrochemistry between cytochromes and Fe(III) oxide electrodes, and is intended as a comparative baseline for subsequence studies of outer membrane cytochromes from dissimilatory iron reducing bacteria (DIRB).

3. Experimental

3.1. Hematite powders for sorption experiments

Hematite was synthesized following Sugimoto et al. [40], and the structure was confirmed using XRD. The resulting thin platelets had a diameter of 1–2 μm and a BET specific surface area of 4.8 $m^2\ g^{-1}$. Hematite was washed three times with 1 M KCl and again with 0.01 M KCl to obtain a 0.01 M KCl background electrolyte (Khare et al. [41]) and stored as stock suspension of 94.1 g hematite kg^{-1} solids concentration.

3.2. Aqueous sorption experiments

Aqueous solutions (KCl, HCl, KOH at 0.01 M and Mcc at 0.1 mM) were prepared using analytical grade reagents and degassed, deionized water. All samples had 1.50 g kg^{-1} suspended solids, ionic strength of 0.01 M KCl, and total mass of 30 ± 0.01 g. Samples were made by weighing out 0.478 g of hematite and adding 0.01 M KCl to about 30% of the final mass; 5000 μL of 0.1 mM Mcc solution was then added, and the pH was adjusted using 0.01 M HCl or 0.01 M KOH before each sample was brought to its final mass. Sample headspace was flushed with N_2. After each experiment, tubes were centrifuged at $\sim 6000 \times g$ for 10 min and the supernatant solution was decanted and analyzed. The pH was measured in a portion of the supernatant solution before filtering, and the remaining solutions were filtered using 0.2-μm polycarbonate filter membranes. Dissolved Mcc concentration was measured using absorbance at 480 nm; this is a longer wavelength than the Soret band peak at 408 nm and is less sensitive to subtle variations in Soret band peak position. The amount of Mcc sorbed on hematite was taken as the difference between total added Mcc and Mcc measured in supernatant solutions after each sorption experiment.

3.3. Electrochemical characterization using hematite electrodes

Hematite (α-Fe_2O_3) from Tarascon sur Ariège, France was used as working electrodes. As received, these crystal surfaces were contaminated with a discontinuous coating of probable goethite (α-FeOOH) particles [42]. These were removed readily, along with contaminating organic matter, using a 1–2 min boil in nitric acid, followed by a brief rinse in concentrated NaOH and rinsing with filtered DDI water. This hematite has an electron donor impurity concentration (mostly Sn and Ti) of about 2.0×10^{-3} at.% based on ICP–MS analyses [42]. Cyclic voltammetry (CV) was conducted using this hematite as working electrodes, a platinum counter electrode, and either an Ag/AgCl reference electrode or an oxidized silver wire calibrated against an Ag/AgCl reference electrode as a pseudo reference. CV experiments took place using 0.1 M KCl solutions, with or without added Mcc. The electrochemical cell was stirred and purged of oxygen using flowing ultra high purity nitrogen gas. CV was performed using an EG&G 263A potentiostat controlled from a PC. Cleaned hematite crystals were attached to a metal clip

and suspended in the solution of interest. Thus, the CV results are not unique to a particular crystal face. The fragile crystals frequently broke while changing solutions, and the total area of the crystal exposed to solution varied with changes in solution, so the absolute magnitudes of current are not necessarily comparable from experiment to experiment. However, the presence or absence, and position, of redox waves is comparable between experiments.

3.4. Atomic force microscopy (AFM)

AFM imaging of Mcc sorbed on hematite (0 0 1) surfaces was done using a Digital Instruments Nanoscope IIIa operating in both contact and AC imaging modes. The same hematite samples were used as electrodes and in AFM observations. We used etched silicon tips/cantilevers with an Al coating to enhance reflectivity.

4. Results

The pH dependence of Mcc sorption to hematite particles in aqueous suspension is given in Fig. 2. The point of zero net charge of the hematite surface occurs at about pH 8.5, and the isoelectric point of the Mcc is at about pH 10. Thus, opposite electrostatic charge on hematite and Mcc only occurs between pH 8.5 and 10. This pH range coincides closely with the peak in adsorption density in Fig. 2, suggesting that the primary sorption interaction is electrostatic. However, van der Waals attractive forces also probably play a role in attracting Mcc molecules to the surface under conditions of very small (or zero) electrostatic repulsion.

Fig. 3 compares the voltammogram of a bare hematite electrode in 0.1 M KCl with that of hematite in the 0.1 mM Mcc solution at pH 7. Redox waves are evident; half-wave potentials for this experiment are listed in Table 1 along with the redox potentials of Mcc from selected literature examples. Our redox potential for Mcc interacting with hematite electrodes is directly comparable to those of other studies (cited above) using oxide electrodes. The form of the voltammogram in Fig. 3 is virtually identical to that reported by Sallez et al. [25] for Mcc interacting with a goethite-modified PG electrode. There is no electrochemical evidence for unfolding or denaturation upon interaction of Mcc with the hematite electrode. Fig. 4 compares the results of an experiment at pH 7 with one at pH 9.5 (this hematite crystal was smaller than the previous one, resulting in lower currents). The current is slightly greater at pH 9.5 than at pH 7, consistent with a greater tendency for the positively charged heme groove to be oriented toward the surface at pH 9.5 than at pH 7 (given a point of zero charge of the hematite surface near pH 8.5). Because these experiments were done with an Ag wire

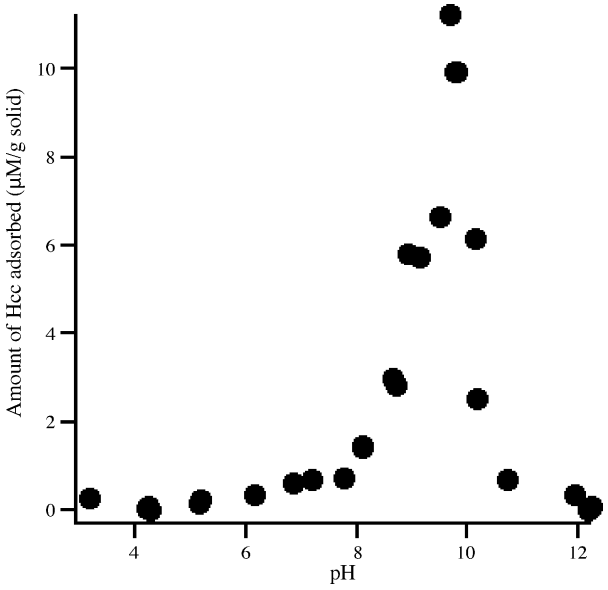

Fig. 2. The pH dependence of Mcc sorption to hematite particles in aqueous suspension. The pH region of greatest sorption corresponds closely to the pH region of opposite charge on hematite (negative above pH 8.5) and Mcc (positive below pH 10).

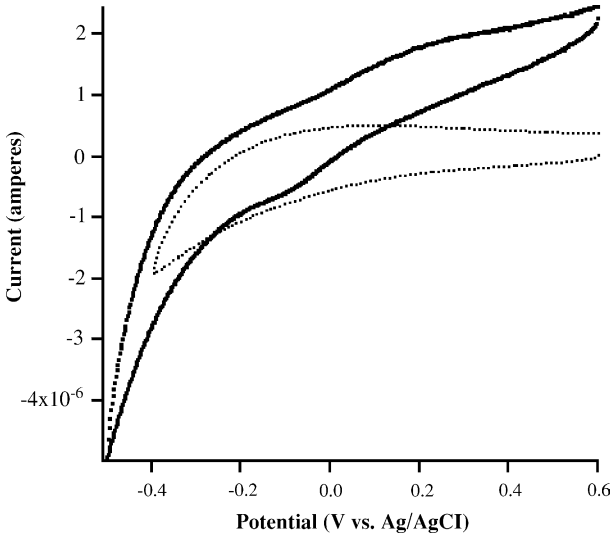

Fig. 3. Voltammogram of Mcc (0.1 mM, 0.1 M KCl) using a hematite electrode (solid line) and of KCl solution without Mcc (dotted line). Because the electrode contact area is different in these two experiments, currents are not directly comparable.

Table 1
Redox potentials for Mcc on different electrode types

Electrode type	Redox potential[a]
Hematite (this work) pH 7, Ag/AgCl[b]	40
Hematite (this work) pH 7, Ag wire[b]	~25
Hematite (this work) pH 9.5, Ag wire[b]	~10
SnO_2 [23]	−30
SnO_2 [24]	55
In_2O_3 [24]	55
Alkanethiol-N^+CH_3 on Au [32]	130
Alkanethiol-CH_2-CH_3 [32]	−320
Alkanethiol-COOH [32]	40
Goethite coated PG[c] [25]	58
4,4′-Bipy on Au [33]	−38

[a] Redox potential is taken as the midpoint between reduction and oxidation waves, mV vs. Ag/AgCl).
[b] Reference electrodes in different hematite experiments are given.
[c] PG, pyrolytic graphite electrode.

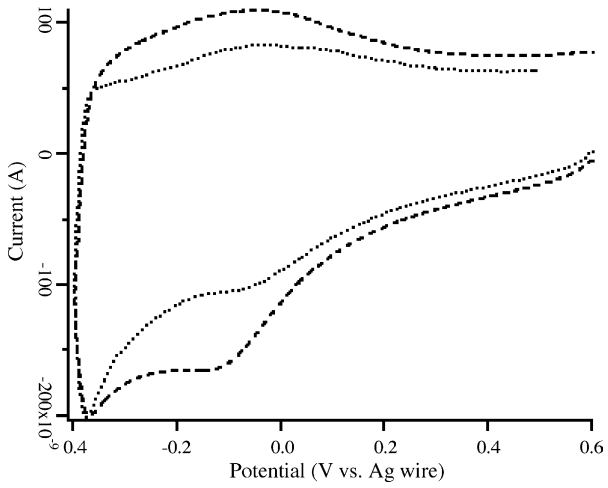

Fig. 4. Voltammogram of Mcc (0.1 mM, 0.1 M KCl) using a hematite electrode at two different pH values. Dotted line: pH near 7; dashed line: pH 9.5.

as a pseudo-reference electrode, the potentials are not directly comparable to those of Fig. 3. However, our calibration of the Ag wire against Ag/AgCl suggests that the corrected potentials should be about 100 mV higher, at 10 mV for pH 9.5 and 25 mV for pH 7. Again, despite uncertainty, these results are comparable to previous results for Mcc interaction with oxide electrodes. The reduction wave at pH 9.5 is slightly negative of the reduction wave for pH 7, possibly indicating that a small amount of Mcc is starting to unfold under high pH conditions (Mcc unfolds above pH 10 [43]).

AFM imaging (in AC mode) is presented in Fig. 5. In the image of a hematite surface in KCl, before addition of Mcc (Fig. 5A), some scratches and a few likely inorganic contaminant particles are evident along with some well-defined steps. Phase-lag imaging (data not shown) suggests that the particles are not fundamentally different from the surrounding surface with regard to adhesive or damping interaction with the oscillating tip. After addition of Mcc (Fig. 5B), the surface appears populated with a larger number of particles. These particles are up to 2.5 nm high relative to the surrounding surface (though many are not so high) and 20–60 nm wide. In contact-mode imaging, these particles are easily swept aside, and the images are highly streaky (Fig. 6). At a low contact force (1–2 nN), streaky images such as that in Fig. 6A are obtained. By increasing contact force to several hundred nanonewtons, an image of a clean surface is produced (Fig. 7A). When contact force is again reduced to a few nanonewtons, and scan area increased, the area scanned at high force (during which sorbed Mcc is swept aside) becomes visible as a scan field in the larger image (Fig. 6B). Both in contact and AC imaging modes, the particles vary from about 1.0–2.5 nm high, and are up to 60 nm wide. These results suggest that the 3.4 nm (diameter) native Mcc molecules are either being perturbed by the AFM imaging (whether or not the AC imaging mode is used) or have changed physical dimensions as a result of adsorption. The fact that we observe native-like redox potentials suggests that no unfolding takes place on the surface, leading us to conclude that the AFM dimensions reflect an imaging artifact. The adsorbed Mcc molecules also probably occur as small aggregates.

Fig. 7A shows an 1 μm × 1 μm area after it had been cleared of sorbed Mcc by high force scanning in contact mode. In this imaging session a 100 mM ammonium phosphate solution was used. Phosphate interacts with Mcc, and dissociation constants are known for three different phosphate binding sites on Mcc [44]. Phosphate also sorbs coordinatively to iron oxides and hydroxides [41]. We hypothesized that Mcc would adhere more strongly to hematite in the presence of phosphate. Fig. 7B shows a nearby area, also after clearing, in which some Mcc has apparently remained attached to steps. This result suggests that steps either hold a greater electrostatic attraction for the Mcc molecules or that there is coordinative attachment of the molecules to steps, perhaps via phosphate "linker" molecules.

Finally, the images in Fig. 5 were taken in circumneutral pH KCl, and the images in Fig. 6 were taken at pH 9.5; as expected, there is greater apparent surface coverage in the high pH images

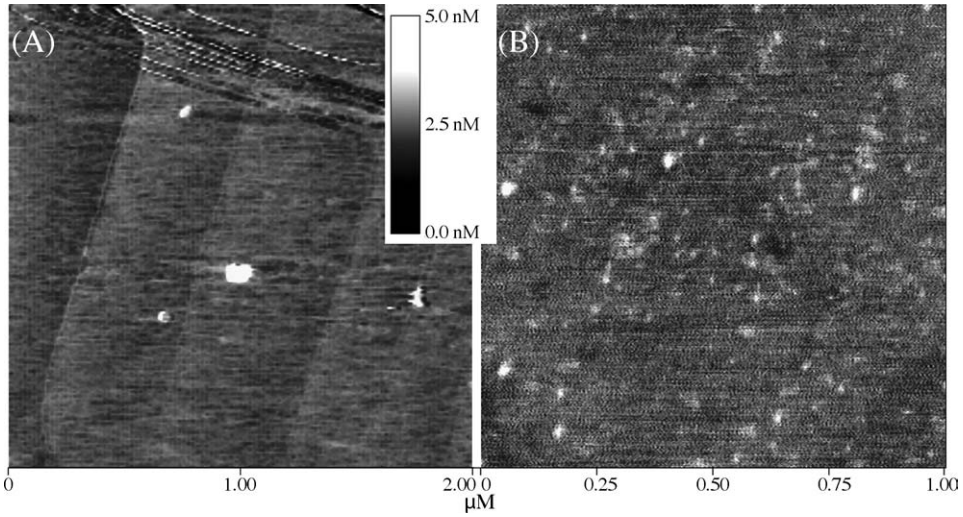

Fig. 5. AC (oscillating cantilever) AFM images of hematite surface without (A) and with (B) sorbed Mcc. Inset: vertical grayscale applies to both images. Image scales are in micrometers.

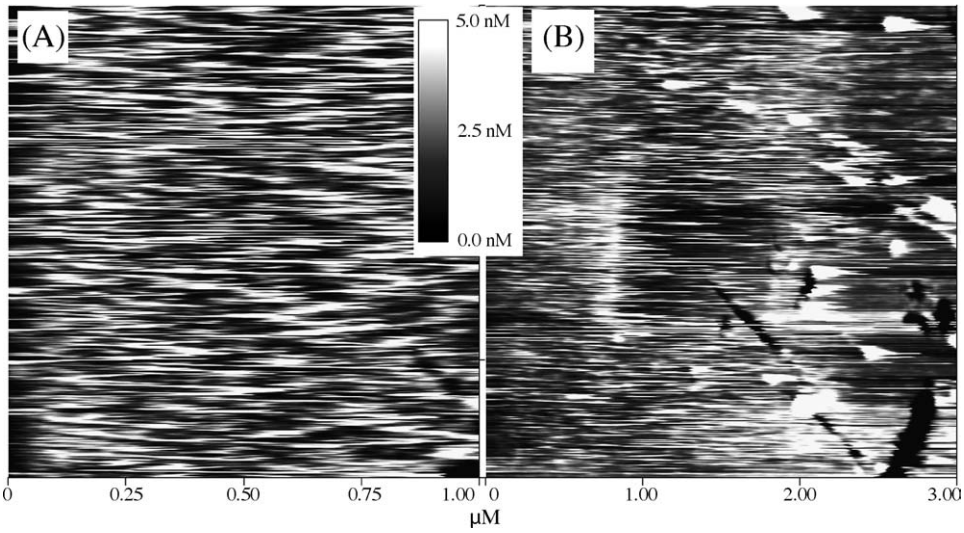

Fig. 6. Contact mode AFM images of a hematite surface in 0.1 mM Mcc solution, pH 9.5. (A) Image taken at low contact force (1–2 nN). (B) Image taken at low force after a high-force scan was taken near the center of the image area. Mcc had been cleared away from the central scan field, and is in the process of resorbing from the Mcc solution in which the imaging was performed.

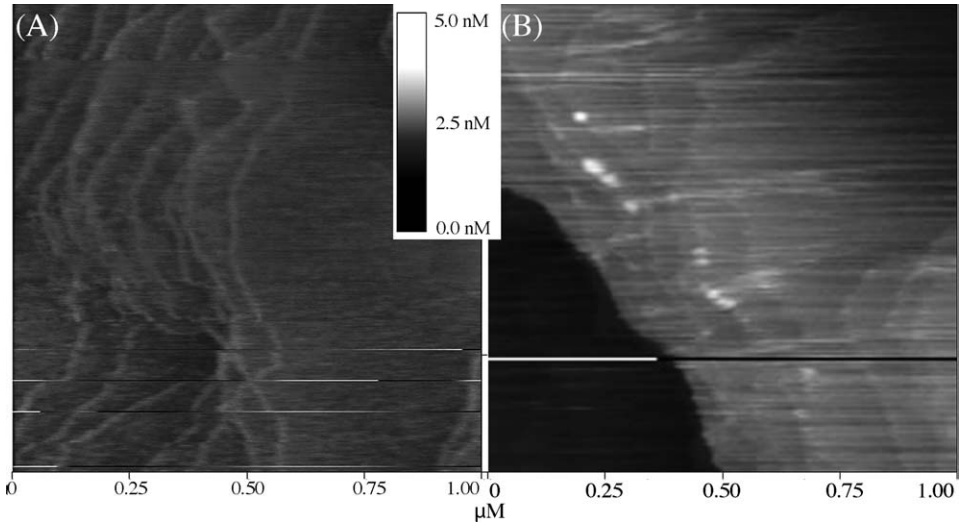

Fig. 7. (A) AFM images taken in 0.1 mM phosphate with 0.1 mM Mcc after a high force (∼200 nN) scan to clear the area of Mcc. (B) High force AFM scan under the same conditions at in (A), showing Mcc molecules adhering to step edges.

than at neutral pH, consistent with the results presented in Fig. 2.

5. Discussion

The aqueous sorption results are generally consistent with electrostatic attraction between the soluble Mcc molecule and the hematite surface, perhaps enhanced by weak van der Waals forces of attraction under pH conditions slightly outside the pH range of expected electrostatic attraction between Mcc molecules and the hematite surface. The cyclic voltammetry results indicate that little or no unfolding of the Mcc molecule occurs upon interaction of Mcc with the hematite electrode surface, and that the molecules are oriented such that electron exchange with the hematite surface is possible. This is expected; the conditions of maximum sorption density (Fig. 2) occur when the hematite surface is negatively charged and thus likely to attract the positive edge of the Mcc dipole (Fig. 1). The positive edge of the Mcc dipole is near the heme groove, which brings the Fe of the heme in Mcc relatively close to the hematite surface. The very low currents associated with the redox waves are probably in part the result of rather small electrode–solution contact areas (on the order of 40 mm^2) as well as the relatively weak electric field at the hematite surface. Any molecules not oriented with the heme as close as possible to the surface will be less able to participate in electron exchange with the hematite electrode, resulting in overall lower currents.

The AFM imaging is consistent with loosely sorbed Mcc molecules not likely to be coordinatively bonded to the surface. Contact mode AFM imaging can easily displace molecules, even at the lowest contact forces. While imaging in aqueous solution,

we found that Mcc resorbed in scan fields within two or three scans (~5 min).

It is likely that some of the large particles (Figs. 5B, 6 and 7B) are aggregates of two or more Mcc molecules. A single unperturbed 3.4 nm diameter molecule, imaged using a tip with a 10 nm radius of curvature, would give an apparent width of about 16 nm. Pressure on the molecule by the tip would likely flatten the molecule somewhat (which is consistent with our AFM data) and make it appear a few nm wider, perhaps 17 or 18 nm wide. However, 60 nm wide particles are inconsistent with single molecules are thus probably results from small aggregates of Mcc molecules. In addition, as Figs. 5B and 7B show, the large particles are relatively few compared to the smaller particles that are about 1.5 nm high and whose width is roughly consistent with a single molecule (17–20 nm) that has been flattened by pressure from the AFM tip on its downswing during AC imaging. Aggregates are expected, especially at pH values close to the isoelectric point of Mcc (pH 10) at which repulsive forces between Mcc molecules are at a minimum and van der Waals attractions can lead to aggregation.

In general, Mcc sorption and electrochemical behavior on hematite electrodes are similar to that on other oxide and oxide-modified electrodes. This result gives us a baseline not only for cytochrome behavior on iron oxide, but perhaps more importantly helps establish hematite as a viable electrode material for direct electrochemistry of cytochromes, including future investigations of outer membrane cytochromes from DIRB.

The future study of cytochrome–mineral interaction will benefit from techniques that provide information about protein molecular and electronic structure while in the sorbed state. A particularly interesting technique, resonant tunneling through redox centers using electrochemical scanning tunneling microscopy [45–47], has the potential to provide electrochemical information from individual molecules and thus allow us to resolve the relationships between location of sorption (e.g., step versus terrace) and molecular redox properties.

6. Conclusions

Aqueous sorption experiments show that extensive adsorption of Mcc to hematite occurs in a narrow pH range (about pH 8.5–10) that corresponds to conditions of oppositely charged hematite surfaces (negative above pH 8.5) and Mcc molecules (positive below pH 10). This result strongly suggests that Mcc sorption to hematite is primarily electrostatically controlled. Cyclic voltammetry investigations show that the electrochemical behavior of Mcc near hematite electrode surfaces is similar to that of the protein in the native confomational state, and similar to the behavior of Mcc on other oxide electrodes (e.g., SnO_2, In_2O_3). In situ AFM imaging is consistent with the wet-chemical results, showing qualitatively that Mcc is in generally loosely attached to the hematite (0 0 1) surface, and that Mcc molecules likely sorb both as individual molecules and as small aggregates. Overall, the results show that Mcc behavior on hematite electrodes is comparable to its behavior on other oxide electrodes. This is important because it suggests that studies of outer membrane cytochromes from DIRB may be performed using both hematite and other oxide electrodes.

Acknowledgements

The authors gratefully acknowledge support from the National Science Foundation grants EAR-987530 and OCE-0434019. Two anonymous reviewers greatly aided revision of the manuscript.

References

[1] R. Hardison, Am. Scientist 87 (2002) 126.
[2] T.A.K. Freitas, J.A. Saito, S. Hou, M. Alam, J. Inorg. Biochem. 99 (2005) 23.
[3] C.E. Castro, R.S. Wade, N.O. Belser, Biochem. 24 (1985) 204.
[4] M. Wirtz, J. Klucik, M. Rivera, J. Am. Chem. Soc. 122 (2000) 1047.
[5] L. Gorton, A. Lindgren, T. Larsson, F.D. Munteanu, T. Ruzzas, I. Gazaryan, Anal. Chim. Acta 400 (1999) 91.
[6] D. Cao, P. He, N. Hu, Analyst 128 (2003) 1268.
[7] J. Deere, M. Serantoni, K.J. Edler, B.K. Hodnett, J.G. Wall, E. Magner, Langmuir 20 (2004) 532.
[8] E. Topoglidis, C.J. Campbell, A.E.G. Cass, J.R. Durrant, Langmuir 17 (2001) 7899.
[9] E. Topoglidis, C.J. Campbell, E. Palomares, R. Durrant, Chem. Commun. 2002 (2002) 1518.
[10] K.J. McKenzie, F. Marken, Langmuir 19 (2003) 4327.
[11] J.K. Fredrickson, J.M. Zachara, D.W. Kennedy, M.C. Duff, Y.A. Gorby, S.-M.W. Li, K.M. Krupka, Geochim. Cosmochim. Acta 64 (2000) 3085.
[12] C. Liu, Y.A. Gorby, J.M. Zachara, J.K. Fredrickson, C.F. Brown, Biotechnol. Bioeng. 80 (2002) 637.
[13] J.R. Lloyd, F.R. Livens, D.R. Lovley, J. Chesnes, S. Glasauer, D.J. Bunker, Geomicrobiol. J. 19 (2002) 103.
[14] H.D. Holland, Geochim. Cosmochim. Acta 66 (2002) 3811.
[15] M. Vargas, K. Kashefi, E.L. Blunt-Harris, D.R. Lovley, Nature 395 (1998) 65.
[16] J.F. Banfield, K.H. Nealson (Eds.), Geomicrobiology: Interactions Between Microbes and Minerals, Reviews in Mineralogy, vol. 35, Mineralogical Society of America, Washington, DC, 1997.
[17] G.E. Brown, V.E. Henrich, W.H. Casey, D.L. Clark, C.M. Eggleston, A. Felmy, D.W. Goodman, M. Gratzel, G. Maciel, M.J. McCarthy, K. Nealson, D.A. Sverjensky, M.F. Toney, J.M. Zachara, Chem. Rev., 99 (1999) 77.
[18] A.S. Beliaev, D.A. Saffarini, J. Bacteriol. 180 (1998) 6292.
[19] S. Gaspard, F. Vazquez, C. Holliger, Appl. Environ. Microbiol. 64 (1998) 3188.
[20] J.M. Myers, C.R. Myers, Biochim. Biophys. Acta 1373 (1998) 237.
[21] T.S. Magnuson, N. Isoyama, A.L. Hodges-Myerson, G. Davidson, M.J. Maroney, G.G. Geesey, D.R. Lovley, Biochem. J. 359 (2001) 147.
[22] C.R. Myers, J.M. Myers, Lett. Appl. Microbiol. 37 (2003) 254.
[23] P. Yeh, T. Kuwana, Chem. Lett. (1977) 1145.
[24] E.F. Bowden, F.M. Hawkridge, H.N. Blount, J. Electroanal. Chem. 161 (1984) 355.
[25] Y. Sallez, P. Bianco, E. Lojou, J. Electroanal. Chem. 493 (2000) 37.
[26] D. Keilin, Proc. R. Soc. London, B Biol. Sci. 98 (1925) 312.
[27] H. Theorell, A. Akesson, J. Am. Chem. Soc. 63 (1941) 1804.
[28] T.J.T. Pinheiro, Biochim. 76 (1994) 489.
[29] L.A. Dick, A.J. Haes, R.P. Van Duyne, J. Phys. Chem. 104 (2000) 11752.
[30] M.R. Gunner, B. Honig, in: R.A. Scott, A.G. Mauk (Eds.), Cytochrome *c*: A Multidisciplinary Approach, University Science Books, Sausalito, 1996, p. 347.
[31] R.E. Dickerson, R. Timkovich, in: P. Boyer (Ed.), The Enzymes, vol. 11, Academic Press, New York, 1975, p. 397.
[32] X. Chen, R. Ferrigno, J. Yang, G.M. Whitesides, Langmuir 18 (2002) 7009.

[33] M.J. Eddowes, H.A.O. Hill, J. Chem. Soc. Chem. Commun. (1977) 771.
[34] S. Boussaad, N.J. Tao, R. Arechabaleta, Chem. Phys. Lett. 280 (1997) 397.
[35] D. Pilloud, X. Chen, P.L. Dutton, C.C. Moser, J. Phys. Chem. B 104 (2000) 2868.
[36] L.J.C. Jeuken, Biochim. Biophys. Acta 1604 (2003) 67.
[37] E. Lojou, P. Bianco, M. Bruschi, Electrochim. Acta 43 (1998) 2005.
[38] E. Lojou, P. Bianco, M. Bruschi, J. Electroanal. Chem. 452 (1998) 167.
[39] T.S. Magnuson, N. Isoyama, A.L. Hodges-Myerson, G. Davidson, M.J. Maroney, G.G. Geesey, D.R. Lovley, Biochem. J. 359 (2001) 147.
[40] T. Sugimoto, A. Muramatsu, K. Sakata, D. Shindo, J. Colloids Interface Sci. 158 (1992) 420.
[41] N. Khare, D. Hesterberg, S. Beauchemin, S.-L. Wang, Soil Sci. Soc. Am. J. 68 (2004) 460.
[42] C.M. Eggleston, A.G. Stack, K.M. Rosso, S.R. Higgins, A.M. Bice, S.W. Boese, R.D. Pribyl, J.J. Nichols, Geochim. Cosmochim. Acta 67 (2003) 985.
[43] F. Boffi, A. Bonincontro, S. Cinelli, A.C. Castellano, A. De Francesco, S. Della Longa, M. Girasole, G. Onori, Biophys. J. 80 (2001) 1473.
[44] G.W. Pettigrew, G.R. Moore, Cytochromes *c* Biological Aspects, Springer-Verlag, New York, 1987.
[45] N.J. Tao, Phys. Rev. Lett. 76 (1996) 4066.
[46] W. Schmickler, N.J. Tao, Electrochim. Acta 42 (1997) 2809.
[47] E.P. Friis, J.E.T. Andersen, Y.I. Kharkats, A.M. Kuznetsov, R.J. Nichols, J.D. Zhang, J. Ulstrup, Proc. Natl. Acad. Sci. U.S.A. 96 (1999) 1379.